Excitation transfer cross sections for levels of the Ne $2p^5 3d$ configuration

John B. Boffard, M. D. Stewart, Jr., and Chun C. Lin
Department of Physics, University of Wisconsin, Madison, Wisconsin 53706
(Received 5 December 2001; revised manuscript received 20 February 2002; published 28 May 2002)

We have measured electron-impact optical emission cross sections for selected resonance and nearby nonresonant levels of the neon $2p^5 3d$ configuration at pressures from 2 to 70 mTorr. The enhanced fluorescence observed from nonresonant levels at high pressures is consistent with excitation transfer from highly populated resonance levels of the $2p^5 3d$ configuration. We measured excitation-transfer cross sections of 540 ± 80 Å^2, 1600 ± 500 Å^2, and 1100 ± 200 Å^2 for transfer from the $3d_5 \rightarrow 3d_6$, $3s_1' \rightarrow 3s_1''$, and $3s_1' \rightarrow 3s_1'''$, respectively.

DOI: 10.1103/PhysRevA.65.062701 PACS number(s): 34.80.Dp, 34.80.My, 33.50.Hv

I. INTRODUCTION

The decay of an isolated excited-state atom is solely via the radiative channel. For a collection of atoms, however, an excited-state atom can also change internal states nonradiatively via collisions with other atoms. Indeed, excitation transfer of energy from one atom to another is the key process in many gas discharge lasers such as the ubiquitous HeNe laser and eximer lasers. In addition to collisions between dissimilar atoms (as in the HeNe laser system), excitation-transfer collisions between excited state and ground-level atoms of the same atomic species are also relevant in the modeling and understanding of plasma kinetics [1–4]. For example, intramultiplet excitation-transfer collisions among the ten levels of the Ne $2p^5 3p$ configuration result in altered optical emission intensities relative to the expected intensities based upon only the populating electron-impact excitation kinematics [1].

Collision transfer cross sections have been extensively studied experimentally for the ten $2p^5 3p$ levels of neon (the $2p$ levels in Paschen's notation) [2,5,6]. In these experiments, a tunable dye laser was used to pump atoms into a selected $2p_i$ level from an atom initially in an excited state of the $2p^5 3s$ configuration, and the increased fluorescence from the decay of a $2p_j$ level was used to deduce the $2p_i \rightarrow 2p_j$ excitation-transfer cross section. With a narrow-band laser and high-resolution optical detection system, one can select both the initial and final states of the excitation-transfer process.

Unfortunately, electric-dipole selection rules and experimental difficulties limit the number of levels that can be studied using this technique. For example, starting from the Ne $2p^5 3s$ configuration, parity selection rules prevent laser excitation into the $2p^5 ns$ and $2p^5 nd$ configurations. On the other hand, laser excitation into the $J=1$ levels of these configurations *is* possible from the ground state, but would require a tunable extreme-ultraviolet laser ($\lambda \approx 60$ nm). As a result of these difficulties, only a small subset of possible excitation-transfer processes have been previously studied in the heavy rare gases.

In this work, we use a different technique to measure excitation-transfer cross sections [7]. An electron beam is used to excite atoms from the ground state into *all* possible excited states. At "high" electron energies, there is a substantial difference in the size of direct electron-impact excitation cross sections into resonance levels (i.e., ones connected to the ground state via dipole-selection rules) and nonresonant levels even for levels in the same configuration. The larger cross sections for dipole-allowed excitation processes lead to the formation of larger excited-state populations of resonance levels vs nearby nonresonant levels. As the pressure of the target gas is increased, the large population of atoms in a resonance level is partially transferred via excitation transfer to the nearby nonresonant levels resulting in increased fluorescence from transitions out of the nonresonant levels. Emission intensities from the nonresonant levels are utilized to determine the transfer cross sections.

II. METHOD

The general formalism of our approach follows that of Gabriel and Heddle [8], and our earlier work on excitation transfer in helium [7]. We briefly discuss the optical method for measuring electron-impact excitation cross sections, and then include the influence of collision transfer.

Consider an electron beam of current I passing through a gas target of number density n_0. Some atoms will be excited to level i. We detect these atoms by measuring the number of photons per beam length per unit time, Φ_{ij}, as they decay to some lower level j. The *optical emission cross section* is defined as

$$Q_{ij}^{\mathrm{opt}} = \frac{\Phi_{ij}}{(I/e)n_0}, \tag{1}$$

where e is the fundamental charge. The *apparent cross section* of level i is the sum of all optical emission cross sections from level i to all lower levels. The apparent cross section is so named since, in the absence of nonradiative channels, it appears to be the cross section into level i. It is also "apparent" in the sense that it includes contributions from both direct electron-impact excitation from $0 \rightarrow i$, as well as a *cascade* contribution from excitation into higher levels k followed by $k \rightarrow i$ decay.

We are concerned with collision transfer between a resonance level R and a nonresonant level N. The nonresonant level is populated by direct electron-impact excitation, collision transfer from the resonance level and cascades from

electron-impact excitation into higher lying levels. It is depopulated by collision transfer collisions, and radiative decay to lower lying levels. Thus the rate equation for the number density of atoms in level N, n_N, is

$$\frac{dn_N}{dt}=n_0\left(\frac{I}{e}\right)Q_N^{\mathrm{dir}}+\sum_{k>N}A_{k\to N}n_k+c_{R\to N}n_R$$

$$-c_{N\to R}n_N-\sum_{j<N}A_{N\to j}n_N, \tag{2}$$

where Q_N^{dir} is the direct excitation cross section into the nonresonant level, $c_{a\to b}$ is the average rate of transfer from level a to b through collisions with ground-state atoms, and $A_{a\to b}$ is the transition probability of the a to b transition. The steady-state solution of Eq. (2) is simply

$$n_N=\frac{n_0\left(\frac{I}{e}\right)Q_N^{\mathrm{dir}}+\sum_{k>N}A_{k\to N}n_k+c_{R\to N}n_R}{c_{N\to R}+\sum_{j<N}A_{N\to j}}. \tag{3}$$

Note that the second term in the numerator is sum of the cascades into the level.

The collision transfer rate is equal to the collision transfer cross section σ times the average relative velocity of two atoms and the atomic number density,

$$c_{R\to N}=4n_0\sigma_{R\to N}(RT/\pi M)^{1/2}, \tag{4}$$

where R is the gas constant (8.31×10^7 amu cm^2 s^{-2} K^{-1}), T is the target gas temperature, and M is the atomic mass. The principle of detailed balance requires that the collision transfer rates $c_{R\to N}$ and $c_{N\to R}$ are related by

$$c_{N\to R}=\left(\frac{g_R}{g_N}e^{-\Delta E/kT}\right)c_{R\to N}, \tag{5}$$

where ΔE is the energy difference between the resonance and nonresonant levels, and g_R and g_N are the statistical weights of the resonance and nonresonant levels. For the cases we are interested in, $\Delta E\ll kT$, so the exponential term is nearly one, and thus will be ignored. To further elucidate the dependence of the collision transfer rate on the gas pressure P, which comes from the dependence on the number density n_0, we define

$$\beta_{R\to N}=\frac{1}{P}c_{R\to N}, \tag{6}$$

which is independent of the atomic number density.

To use Eq. (3) to determine the transfer rate, we observe one optical emission cross section, the $N\to l$ transition. The rate of photon emission for this transition per unit electron-beam length, according to Eq. (3) is

$$\Phi_{N\to l}=A_{N\to l}n_0\left(\frac{I}{e}\right)\frac{Q_N^{\mathrm{dir}}+Q_N^{\mathrm{casc}}+P\left(\frac{e}{n_0I}\right)\beta_{R\to N}n_R}{\sum_{j<N}A_{N\to j}+\frac{g_R}{g_N}\beta_{R\to N}P}, \tag{7}$$

where Q_N^{casc} is the cascade cross section, which is equal to the second term in the numerator of Eq. (3) divided by (n_0I/e). The number of atoms in the resonance level, n_R, is found by a separate measurement of the optical emission cross section of the $R\to l'$ transition. Due to radiation trapping, this cross-section measurement, like the case of He($5^1P\to2^1S$) discussed in Ref. [7], exhibits some pressure dependence,

$$n_R=\frac{n_0(I/e)Q_{R\to l'}^{\mathrm{opt}}(P)}{A_{R\to l'}}. \tag{8}$$

Upon substitution of Eq. (8) into Eq. (7) and combining Q_N^{dir} and Q_N^{casc} as the apparent cross section Q_N^{app}, we find that

$$Q_{N\to l}^{\mathrm{opt}}(P)=A_{N\to l}\frac{Q_N^{\mathrm{app}}+P\left(\frac{\beta_{R\to N}}{A_{R\to l'}}\right)Q_{R\to l'}^{\mathrm{opt}}(P)}{\sum_{j<N}A_{N\to j}+\frac{g_R}{g_N}\beta_{R\to N}P}. \tag{9}$$

To extract the collision transfer rate, we take our observed optical cross-section measurements for both the resonance and nonresonant levels as input to Eq. (9). Using the known values of the transition probabilities [9–11], the fit has two free parameters: Q_N^{app}, the apparent cross section (direct plus cascade) into the nonresonant level; and $\beta_{R\to N}$, which is converted into the collision transfer cross section via Eq. (4). In general, the apparent cross section for level N, may also have some pressure dependence due to radiation trapping of cascading levels [12]. For the particular levels studied in this work, the cascade contribution is small and exhibits little pressure dependence [13], which justifies this simplification. However, if the pressure dependence of the cascading levels are known, this effect can be easily included in Eq. (9) by replacing Q_N^{app} with a fitted pressure independent term, Q_N^{dir}, and an experimentally measured pressure dependent cascade term, $Q_N^{\mathrm{casc}}(P)$.

The experimental apparatus and general data collection procedures have been described in detail elsewhere [7,12], thus we present only a brief overview. The stainless steel vacuum chamber is evacuated to a base pressure of $<2\times10^{-8}$ Torr, and then back filled with research purity (99.999%) neon. The gas pressure was measured with a spinning rotor gauge. The monoenergetic electron beam (0.6-eV energy spread) is formed by an indirectly heated BaO cathode, electrostatically focused through the collision region and collected with a deep Faraday cup. Fluorescence from a particular transition was selected with a 1.26-m Czerny-Turner spectrometer and detected with a C31034A photomultiplier tube (PMT). Relative optical emission cross sections are obtained by dividing the emission intensities from the

PMT by the electron-beam current and gas pressure. A relative pressure curve is obtained by measuring the optical emission cross section at a fixed electron-beam energy as a function of gas pressure. An excitation function is the cross section at a fixed pressure as a function of electron-beam energy. The relative results are placed on an absolute scale by comparing the excitation signal intensity at 20 mTorr and 100 eV with the output of a calibrated standard lamp [13].

III. RESULTS

We have studied excitation transfer for three pairs of energy levels of the neon $2p^5 3d$ configuration. The electron-impact excitation cross sections into the three $J=1$ levels of the $2p^5 3d$ configuration ($3s_1'$, $3d_2$, and $3d_5$ in Paschen's notation) are relatively large, with broad excitation functions characteristic of dipole-allowed excitation processes [12]. For example, the average cross section for excitation into the three $2p^5 3d$ levels with $J=1$ at 100 eV is approximately 19×10^{-20} cm^2, whereas the remaining nine levels with $J\neq1$ have an average cross-section value less than 3×10^{-20} cm^2 [13].

The size of an excitation-transfer cross section between two levels, in turn, typically varies inversely with the energy difference between the initial and final energy levels (the energy defect) [14]. Thus the excitation-transfer cross section out of the $2p^5 3d$ $J=1$ levels is expected to be large for all levels with an energy defect much less than kT ($\sim$208 cm^{-1} at 300 K). The smallest energy defects, and correspondingly largest expected collision transfer cross sections are from the $3d_5$ ($J=1$) level into the $3d_6$ ($J=0$) level ($\Delta E=14$ cm^{-1}); and from the $3s_1'$ ($J=1$) level into the $3s_1''$ ($J=2$, $\Delta E=16$ cm^{-1}), $3s_1'''$ ($J=3$, $\Delta E=26$ cm^{-1}), and $3s_1''''$ ($J=2$, $\Delta E=27$ cm^{-1}) levels. Overlapping transitions and weak signal rates prevented us from making measurements for the $3s_1'''$ level. The same difficulties occur in the case of the $3d_2$ ($J=1$)/$3d_3$ ($J=2$) pair that are separated by only 30 cm^{-1}.

Let us consider first the transfer from the dipole-allowed $3d_5$ level into the $3d_6$ level. We plot in Fig. 1 the measured variation in the $3d_6\rightarrow2p_{10}$ optical emission cross section with pressure at an electron energy of 100 eV. Below 10 mTorr there is little dependence of the cross section with pressure, but at higher pressures the cross section increases almost linearly with pressure. We fit the data to Eq. (9) using our previously measured $3d_5\rightarrow2p_{10}$ optical emission cross section [12] and the transition probabilities of Ref. [11]. The line in Fig. 1 is the fit to the data with a collision transfer cross section of 5.4×10^{-14} cm^2.

Neon is not an *LS* coupled atom so that the wave function for a level of total angular momentum *J* is in general a mixture of *LS* eigenfunctions of the same *J*. However, since the $3d_6$ level is the only $2p^5 3d$ level with $J=0$, it is a pure triplet level ($^3P_0$) within the one-configuration approximation. Direct electron-impact excitation into the $3d_6$ level from the $^1S_0$ neon ground state thus corresponds to a spin-changing process dominated by a steep-declining energy dependence. The observed energy dependence of the $3d_6$ excitation cross section *at high pressures* as shown in Fig. 2, however, has the broad energy dependence of a dipole-allowed excitation process. This is due to excitation transfer from the $3d_5$ level whose electron-impact excitation is dipole allowed. For example, at 50 mTorr, the $3d_6\rightarrow2p_{10}$ cross section decreases only 32% between 50 eV and 200 eV. At low pressures, however, the observed energy dependence of the cross section is much sharper, with a 90% decrease between 50 eV and 200 eV. The observed energy dependence at both pressure extremes is well modeled by Eq. (9) using the known $3d_5\rightarrow2p_{10}$ excitation function and the fitted values for the apparent excitation cross section and collision transfer cross section.

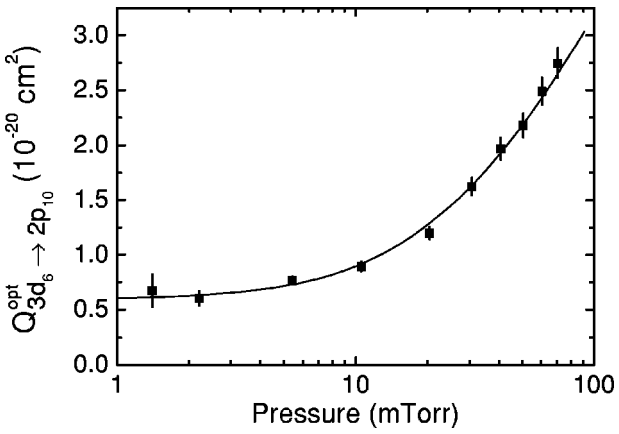

FIG. 1. Variation of $3d_6\rightarrow2p_{10}$ optical emission cross section at 100 eV with pressure. The solid line is a fit of Eq. (9) to data using the measured pressure dependent $3d_5\rightarrow2p_{10}$ optical emission cross section.

The situation of excitation transfer from the $3s_1'$ level is somewhat different since it is in close proximity to three other levels ($3s_1''$, $3s_1'''$, and $3s_1''''$). In fact all four of the $3s_1$ levels are spaced within 27 cm^{-1} of one another, thus the collision transfer cross section between any pair of levels

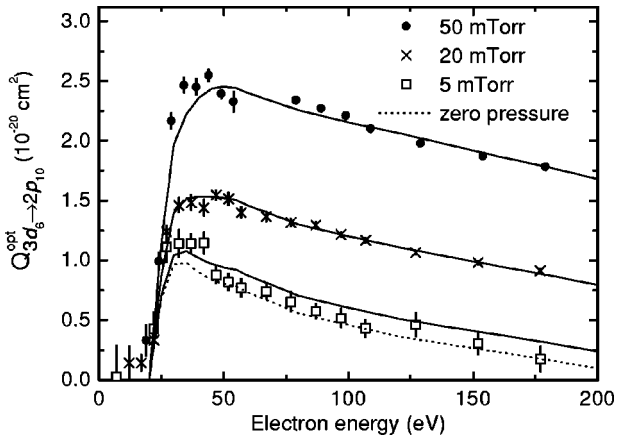

FIG. 2. Excitation functions for the $3d_6\rightarrow2p_{10}$ transition at different pressures. The solid lines are the results of using Eq. (9) along with the fitted $3d_6$ apparent cross section and $3d_5\rightarrow3d_6$ excitation-transfer cross section. The dotted line is the $3d_6\rightarrow2p_{10}$ optical emission cross section derived from Eq. (9) in the limit of no collision transfer.

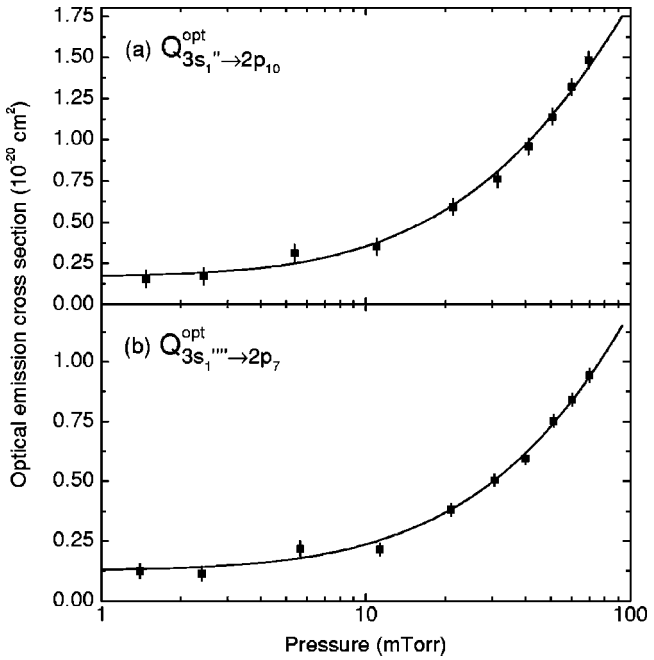

FIG. 3. Variation of $3s_1''\rightarrow 2p_{10}$ and $3s_1''''\rightarrow 2p_7$ optical emission cross sections at 100 eV with pressure. Solid lines are a fit of Eq. (9) to data using the measured pressure dependent $3s_1'\rightarrow 2p_{10}$ optical emission cross section.

may be large. The analysis of Sec. II, however, included only collision transfer directly from the $3s_1'$ resonance level. In principle, Eq. (2) can be modified to include collision transfer to and from additional levels. However, the electron-impact excitation cross sections into the three $J\neq 1$ $3s_1$ levels are of similar magnitude [13], leading to roughly equal populations for the three levels. Since the ratio of collision transfer rates for $a\rightarrow b$ to $b\rightarrow a$ is equal to $(2J_b+1)/(2J_a+1)\approx 1$, the total flow of atoms between any pair of levels of nearly equal population is negligible in comparison to the population flow from the $J=1$ $3s_1'$ level with a cross section/population greater than a factor of 10 larger than the other levels. Another omission in our model developed in Sec. II relevant to the $3s_1''''$ level is collision transfer via an intermediate state, e.g., $3s_1'\rightarrow 3s_1''\rightarrow 3s_1''''$. Such a two-step process, however, has a quadratic rather than linear dependence on pressure. Based on the measurements of Ref. [2] for neon $2p^5 3p$ two-step collision transfer, we are well below the pressures where this is of serious importance.

Pressure curves for the $3s_1''$ and $3s_1''''$ levels are shown in Fig. 3. The solid lines shown in Fig. 3 are the result of fitting Eq. (9) to the data. The reasonable agreement of the fits gives us confidence about the validity of our omitting the terms mentioned in the preceding paragraph. The fitted collision transfer cross sections for the three processes studied in this paper are listed in Table I. The largest sources of uncertainty in the fitted values are from the transition probabilities (particularly $A_{R\rightarrow l'}$).

IV. DISCUSSION

It is interesting to compare the present $2p^5 3d$ intramultiplet collision transfer cross sections with the previously measured $2p^5 3p$ intramultiplet values determined in Refs. [2,5,6]. The smallest energy defect for levels of the $2p^5 3p$ configuration is between the $2p_3$ and $2p_4$ levels with an energy defect of 59 cm^{-1} (8 meV). Paterson *et al.* [2] measured the cross section for $2p_3\rightarrow 2p_4$ excitation transfer to be 19×10^{-16} cm^2. The $2p^5 3d$ collision transfer cross sections reported in this paper are approximately two orders of magnitude larger, while differing by less than one order of magnitude in energy defects. The present cross section values are similar is size, however, to our earlier measurements of He $n^1P\rightarrow nF$ collision transfer [7], which have similar energy defects.

TABLE I. Thermally averaged (300 K) Ne $2p^5 3d$ excitation transfer cross sections.

Process	ΔE (cm^{-1})	σ (10^{-14} cm^2)
$3d_5\rightarrow 3d_6$ $(J=0)$	14	5.4 ± 0.9
$3s_1'\rightarrow 3s_1''$ $(J=2)$	16	16 ± 5
$3s_1'\rightarrow 3s_1''''$ $(J=2)$	27	11 ± 2

To further elucidate the dependence on energy defect, in Fig. 4 we plot the state-to-state excitation-transfer cross sections obtained by dividing the values in Table I by $(2J+1)$ of the final level. Also included in Fig. 4 are a number of other excitation-transfer cross sections for excited atoms colliding with a similar ground-state atom [2,5–7,15–21]. By plotting the state-to-state cross section, we remove the con-

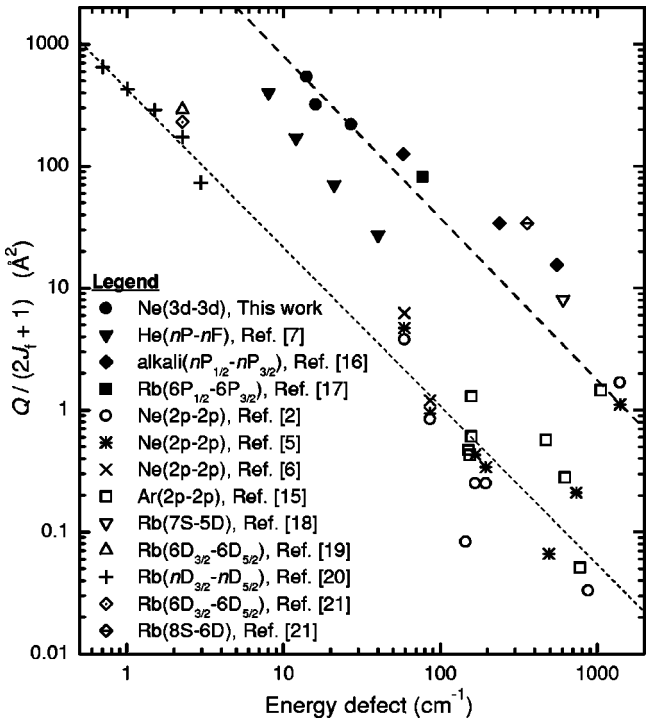

FIG. 4. Comparison of state-to-state excitation-transfer cross sections with energy defect. Solid-filled symbols all involve excitation-transfer processes where the initial level is a resonance level; open symbols are for excitation transfer between nonresonance levels. Dashed lines are only an illustrative guide. The exothermic reaction for each process is plotted.

founding influence of the $(2J+1)$ degeneracy in the final level. Two interesting features are apparent in Fig. 4. First, the magnitude of an excitation-transfer cross section is inversely related to the energy defect for the process. Second, if we group the results shown in Fig. 4 into excitation-transfer processes involving resonance levels (represented by filled symbols) and excitation-transfer processes involving nonresonance levels, the cross sections involving resonance levels are approximately 40 times larger than the cross sections involving only nonresonant levels with the same energy defect.

The two major features of Fig. 4 can be understood from a simple analysis based on the Massey adiabatic criterion for atom-atom collisions [22]. For the case of A-to-B excitation transfer, let us assume the intermolecular potential curves for $A+X$ and $B+X$ have an avoided crossing at a distance a, where X is the ground state. If the collision is adiabatic (i.e., $v \ll a\Delta E/h$, where v is the relative velocity of the atoms, ΔE is the energy defect between levels A and B, and h is Planck's constant), the system remains on the same potential curve for the duration of the collision, and the excitation cross section is small. On the other hand, if the atoms collide at much higher velocities, the system can hop from the $A+X$ potential curve to the $B+X$ one, yielding a cross section on the order of πa^2. For a small energy defect, not only is the Massey velocity criterion more easily satisfied, but it is also more likely that a curve crossing will occur at a larger inter-atomic distance. For collisions involving a resonance level, the difference in the interatomic potentials can scale as $1/r^3$, whereas collisions involving only nonresonance levels will have a weaker dependance on interatomic separation [14]. Thus for a given asymptotic energy defect, a curve crossing can occur at a larger distance—yielding a larger cross section—more readily for collisions involving a resonance level [23]. To extend the qualitative nature of this discussion to a more quantitative level would require a detailed knowledge of the intermolecular potentials for all levels involved. As a result, *ab initio* calculations of excitation cross sections are exceedingly difficult, and have generally been limited to simpler systems [23,24].

The present results use an electron beam as an excitation mechanism to extend previous neon excitation-transfer cross-section measurements [2,5,6] to levels that would otherwise be exceptionally difficult to measure via laser excitation. The major disadvantage of using an electron beam for excitation is that it is nonselective—it is only useful in studying collision transfer between adjacent energy levels which have dramatically different electron-impact cross sections. In this paper, we have applied the method to cases where one level is a resonance level, and one level is a nonresonant level. In principle, however, this restriction is not necessary. For example, it may be possible to study excitation transfer between the krypton $2p_8$ and $2p_9$ levels (which are both nonresonant) since they are nearly degenerate ($\Delta E = 13\ \mathrm{cm}^{-1}$), and have electron-impact excitation cross sections that vary by an order of magnitude at high energies [25].

ACKNOWLEDGMENTS

This work was supported by the Air Force Office of Scientific Research and the National Science Foundation.

[1] W.L. Nighan, IEEE Trans. Electron Devices **28**, 625 (1981).
[2] A.M. Paterson, D.J. Smith, I.S. Borthwick, and R.S. Stewart, J. Phys. B **34**, 1815 (2001).
[3] T. Bräuer, S. Gortchakov, D. Loffhagen, S. Pfau, and R. Winkler, J. Phys. D **30**, 3223 (1997).
[4] A. Bogaerts, R. Gijbels, and J. Vlcek, J. Appl. Phys. **84**, 121 (1998).
[5] R.S.F. Chang and D.W. Setser, J. Chem. Phys. **72**, 4099 (1980).
[6] J.P. Grandin, D. Hennecart, X. Husson, D. LeCler, J.F. Vienne, and M. Barrat-Rambosson, J. Phys. (France) **36**, 787 (1975).
[7] J.E. Chilton and C.C. Lin, Phys. Rev. A **58**, 4572 (1998).
[8] A.H. Gabriel and D.W.O. Heddle, Proc. R. Soc. London, Ser. A **258**, 124 (1960).
[9] NIST Atomic Spectra Database, URL http://physics.nist.gov/asd
[10] R.A. Lilly, J. Opt. Soc. Am. **66**, 245 (1976).
[11] M.J. Seaton, J. Phys. B **31**, 5315 (1998).
[12] M.D. Stewart, J.E. Chilton, J.B. Boffard, and C.C. Lin, Phys. Rev. A **65**, 032704 (2002).
[13] J.E. Chilton, M.D. Stewart, and C.C. Lin, Phys. Rev. A **61**, 052708 (2000).
[14] N.F. Mott and H.S.W. Massey, *The Theory of Atomic Collisions* (Clarendon Press, Oxford, 1965).
[15] R.S.F. Chang and D.W. Setser, J. Chem. Phys. **69**, 3885 (1978).
[16] L. Krause, Appl. Opt. **5**, 1375 (1966).
[17] P.W. Pace and J.B. Atkinson, Can. J. Phys. **52**, 1635 (1974).
[18] L. Caiyan, A. Ekers, J. Klavins, and M. Jansons, Phys. Scr. **53**, 306 (1996).
[19] J. Supronowicz, J.B. Atkinson, and L. Krause, Phys. Rev. A **31**, 2691 (1985).
[20] J.W. Parker, H.A. Schuessler, R.H. Hill, and B.G. Zollars, Phys. Rev. A **29**, 617 (1984).
[21] A. Ekers, M. Głódź, J. Szonert, B. Bieniak, K. Fronc, and T. Radelitski, Eur. Phys. J. D **8**, 49 (2000).
[22] See for example, E.W. McDaniel, J.B.A. Mitchell, and M.E. Rudd, *Atomic Collisions: Heavy Particle Projectiles* (Wiley, New York, 1993).
[23] M. Bouledroua, A. Dalgarno, and R. Côté, Phys. Rev. A **65**, 012701 (2001).
[24] J.S. Cohen, L.A. Collins, and N.F. Lane, Phys. Rev. A **17**, 1343 (1978).
[25] J.E. Chilton, M.D. Stewart, and C.C. Lin, Phys. Rev. A **62**, 032714 (2000).